RSC Advances

PAPER

View Article Online
View Journal | View Issue

Cite this: *RSC Adv.*, 2016, **6**, 36528

Core–spacer–shell structured $NaGdF_4$:Yb^{3+}/Er^{3+}@$NaGdF_4$@Ag nanoparticles for plasmon-enhanced upconversion luminescence†

Xindan Zhang,[ab] Bin Li,*[a] Mingming Jiang,[a] Liming Zhang*[a] and Heping Ma[a]

Received 28th December 2015
Accepted 1st April 2016

DOI: 10.1039/c5ra27881c

www.rsc.org/advances

To increase emission of up-converting materials, $NaGdF_4$:20%Yb^{3+}/2%Er^{3+}@$NaGdF_4$@Ag up-converting nanoparticles (UCNPs) in core–spacer–shell structure have been designed and fabricated. Significant emission enhancement compared with ordinary $NaGdF_4$:20%Yb^{3+}/2%Er^{3+} has been obtained. Furthermore, the enhancement mechanism have been found as the protective effect of $NaGdF_4$ and localized surface plasmon resonance (LSPR) of Ag.

1. Introduction

In recent years, up-converting materials have gathered considerable attention due to their capability of absorbing low-energy light and re-emitting high-energy light *via* a multiple-photon absorption process.[1–3] Additionally, their favorable virtues of less photo damage to living organisms, weaker background fluorescence, and deeper tissue penetration notably open a door to biological applications, such as cell tracking and imaging, fluorescence assays, and therapeutic probes.[4–10] In response to these ever-increasing needs of biological applications, nano-sized up-converting materials with functional structure and hydrophilic nature have been proposed.[11–14] However, the synthesis of up-converting nanoparticles (UCNPs) usually comes at the expense of weak luminescent intensity, which limits their further application. Saying from this situation, extensive work has been carried out to enhance up-converting emission intensity, such as modulating host materials and dopant concentrations,[15,16] coating protective shells,[17] and coupling with noble metals.[18] Unfortunately, the energy efficiency of the most efficient up-converting material, hexagonal (β) phase $NaYF_4$ nanocrystals co-doped with 20% Yb^{3+} and 2% Er^{3+}, is still no more than 4% at pump intensity around 1000 W cm^{-2}.[19] By introducing protective shells such as SiO_2 and coupling with noble metal (Ag/Au), luminescence can be enhanced due to the surface protective effect and Localized Surface Plasmon Resonance (LSPR).[20–23] However, among these studies, a large proportion of products are assembled on glass or imbedded in films, which hardly satisfies biological applications. To realize valid enhancement of luminescent intensity in nano-sized up-converting materials, we present the synthesis of UCNPs with a heterostructure of $NaGdF_4$:Yb^{3+}/Er^{3+}@$NaGdF_4$@Ag. To the best of our knowledge, there are no reports on the combination of homogeneous coating and LSPR with promising luminescent properties for potential biological applications so far.

2. Results

2.1. Synthesis and characterization of $NaGdF_4$:20%Yb^{3+}/2%Er^{3+}@$NaGdF_4$@Ag UCNPs

The stepwise preparation of $NaGdF_4$:20%Yb^{3+}/2%Er^{3+}@$NaGdF_4$@Ag core–spacer–shell UCNPs is presented in Scheme 1. Firstly, core UCNPs of a GdF_4:20%Yb^{3+}/2%Er^{3+} are synthesized according to a modified high temperature thermolysis method. And as-prepared cores are used as seeds to fabricate core–spacer UCNPs of $NaGdF_4$:20%Yb^{3+}/2%Er^{3+}@$NaGdF_4$ *via* homogeneous coating. After that, OA on the surface of core–spacer UCNPs of $NaGdF_4$:20%Yb^{3+}/2%Er^{3+}@$NaGdF_4$ is washed off in a faintly acidic condition to realize the modulation of surface chemical ligand. To introduce metallic nanostructure of Ag, core–spacer UCNPs of

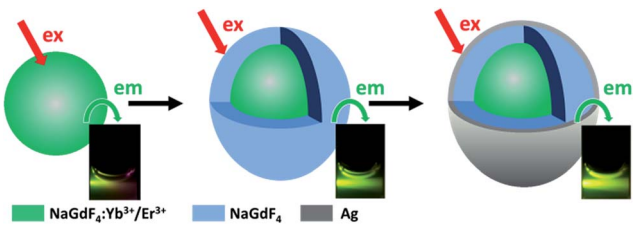

Scheme 1 Synthesis procedure for core–spacer–shell UCNPs of $NaGdF_4$:20%Yb^{3+}/2%Er^{3+}@$NaGdF_4$@Ag.

[a]*State Key Laboratory of Luminescence and Applications, Changchun Institute of Optics Fine Mechanics and Physics, Chinese Academy of Sciences, Changchun 130033, PR China. E-mail: lib020@ciomp.ac.cn*

[b]*University of Chinese Academy of Sciences, Beijing 100049, PR China*

† Electronic supplementary information (ESI) available: Energy diagram and simplified mechanism for energy-transfer up-converting process and FT-IR spectra. See DOI: 10.1039/c5ra27881c

$NaGdF_4$:Yb^{3+}/Er^{3+}@$NaGdF_4$ are functionalized with thiol groups (–SH) by adding TGA which has ability to concentrate Ag^+ on UCNPs surface. Then Ag shell is fabricated onto UCNPs surface after the reduction of Ag^+ by adding AA under the help of sodium citrate which acts as a stabilizer in water solution.[24]

In our case, hexagonal-phase $NaGdF_4$ is chosen as our model host system owing to its merit of small size (<20 nm) to match biological and medical applications.[25] As revealed by their SEM images and corresponding size distribution in Fig. 1, core UCNPs of $NaGdF_4$:20%Yb^{3+}/2%Er^{3+} (Fig. 1a) have an average diameter of about 14 nm, and core–spacer UCNPs of $NaGdF_4$:-Yb^{3+}/Er^{3+}@$NaGdF_4$ (Fig. 1b) show an average diameter of about 17.5 nm which obviously bigger than that of $NaGdF_4$:20%Yb^{3+}/2%Er^{3+}, suggesting the growth of a homogeneous coating spacer. In TEM image (Fig. 1c) of core–spacer–shell UCNPs of $NaGdF_4$:Yb^{3+}/Er^{3+}@$NaGdF_4$@Ag, it is clear that Ag shell is thin with thickness of ~1.5 nm. The diameter of integrate core–spacer–shell UCNPs is about 20 nm. And the distance of 0.3 nm between the adjacent lattices in high-resolution transmission electron microscopy (HRTEM) images (inset of Fig. 1c) agrees well with the *d* 100 spacing (0.301 nm) of hexagonal-phased $NaGdF_4$. Furthermore, energy-dispersive X-ray (EDX) and elemental mapping clearly demonstrate that the element Ag is confined in the UCNPs. Also, elements of Na, F, Gd, Yb and Er corresponding to core UCNPs and core–spacer UCNPs are distributed in the same position. And the XRD result shown in Fig. 2, indicates the existence of $NaGdF_4$ in hexagonal phase and Ag in cubic phase in core–spacer–shell structured UCNPs. The size distribution of core–spacer–shell UCNPs in deionized water by dynamic light scattering (DLS) is presented in Fig. S1† and the average hydrodynamic diameter which is normally bigger than actual size is 171 nm. Maybe some extent of aggregation exists in water.

TGA plays an important role in modifying surface chemical property of UCNPs and enriching their surface with Ag^+. Hence, Fourier-transform infrared (FT-IR) spectra of unmodified UCNPs (UCNPs-OA) and TGA-modified UCNPs (UCNPs-TGA) are shown in Fig. S2† to confirm the surface modification. In Fig. S2,† the differences at 2600 cm^{-1} caused by vibration of –SH could be regarded as direct evidence of HS–CH_2–COOH (TGA) modification.

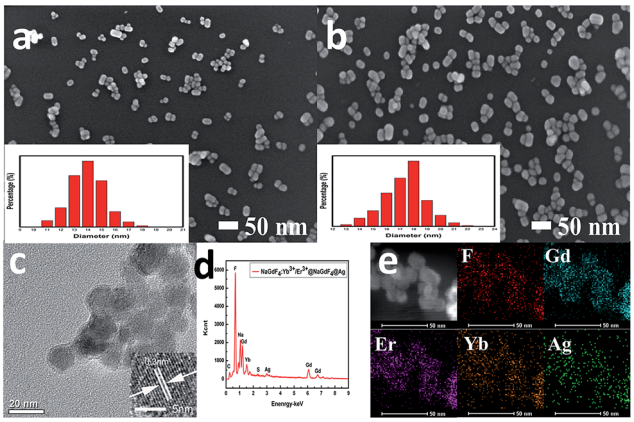

Fig. 1 SEM images of core UCNPs (a) and core–spacer UCNPs (b), insets are their corresponding particles size distribution histograms. Low-resolution (c) and high-resolution (inset of c) TEM images of core–spacer–shell UCNPs, EDX spectra (d) and element mapping (e) of core–spacer–shell UCNPs.

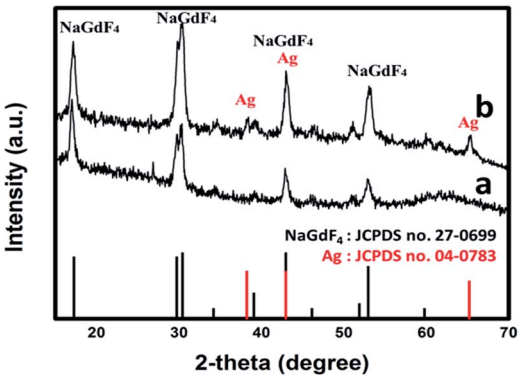

Fig. 2 XRD patterns of core–spacer UCNPs (a) and core–spacer–shell UCNPs (b). The standard data for hexagonal phase $NaGdF_4$ (JCPDS no. 27-0699) and cubic phase Ag (JCPDS no. 04-0783) are shown as references.

Meanwhile, vibration at 3400 cm^{-1}, 2925 cm^{-1}, 2850 cm^{-1}, and 1710 cm^{-1} respectively arising from vibration of –OH, –CH_2, –CH_2, and C=O appear in both spectra given the existence of –COOH in OA and TGA, and notably, vibration peaks of –CH_2 and C=O have blueshift to some degree indicating the more stronger coupling between TGA and UCNPs than between OA and UCNPs. However similar change is not observed at the peak of 3400 m^{-1}, perhaps because –OH is always likely to be affected by external environment and then fail to show a precise change.

2.2. Optical property of $NaGdF_4$:20%Yb^{3+}/2% Er^{3+}@$NaGdF_4$@Ag UCNPs

In our case, Gd^{3+} ions that feature half-filled ^{4}f orbitals are relatively inert in luminescence process and thus have negligible interaction with emitting dopant Er^{3+}.[26] Yb^{3+} ions are introduced into up-converting system, acting as a sensitizer. Up-converting mechanism of the sensitizer–emitter pair Yb^{3+}–Er^{3+} is illustrated in Fig. S3.† Absorption at 980 nm of Yb^{3+} is followed by energy transfer to $^4I_{11/2}$ energy level of Er^{3+}. A second absorption and energy transfer event populates a higher-energy state, which leads to two primary emission bands in visible region at 540 nm (green region) and 650 nm (red region).

For a complete characterization of core–spacer–shell nanostructures on UC luminescence, absorption spectrum of $NaGdF_4$:20%Yb^{3+}/2%Er^{3+}@$NaGdF_4$@Ag is carried out and shown in Fig. 3. It is clear that the core–spacer–shell UCNPs reserve an obvious up-converting property of sensitizer–emitter pair of Yb^{3+}–Er^{3+} peaking at 980 nm.

In our study, the core–spacer–shell UCNPs of $NaGdF_4$:20% Yb^{3+}/2%Er^{3+}@$NaGdF_4$@Ag exhibit excellent up-converting property and enhanced up-converting luminescence owing to the homogeneous coating of $NaGdF_4$ spacer and LSPR of Ag shell. As shown in Fig. 4, photoluminescent spectra of four

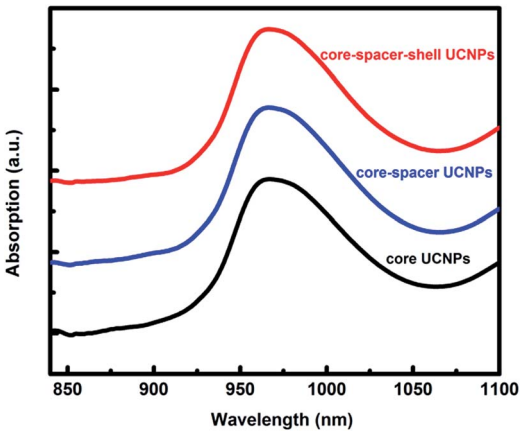

Fig. 3 Absorption spectra of core UCNPs (black line), core–spacer UCNPs (blue line), and core–spacer–shell UCNPs (red line).

UCNPs, which are $NaGdF_4$:Yb^{3+}/Er^{3+}@$NaGdF_4$@Ag UCNPs (spectrum a, sample a), $NaGdF_4$:Yb^{3+}/Er^{3+}@$NaGdF_4$ UCNPs (spectrum b, sample b), $NaGdF_4$:Yb^{3+}/Er^{3+} UCNPs (spectrum c, sample c) and $NaGdF_4$:Yb^{3+}/Er^{3+}@Ag UCNPs (spectrum d, sample d), are discussed below to investigate their up-converting emission enhancement mechanism. Compared to pure core UCNPs (spectrum c), the introductions of $NaGdF_4$ spacer (spectrum b) and Ag shell (spectrum a) do not alter up-converting emission peak and spectral shape, but enhance emission intensity strongly successively. Enhancement factors attributed to homogeneous coating structure are 6.08-fold at 540 nm and 4.73-fold at 650 nm. And enhancement factors attributed to plasmonic coupling of Ag shell are 2.0-fold at 540 nm and 2.51-fold at 650 nm. Moreover, it is noteworthy that all samples dispersed in deionized water contain the same concentration of UCNPs (5 mg mL^{-1}), leading to the gradual decrease of Er^{3+} concentration. Thus enhancement factors are actually higher than above mentioned numbers.

However, UCNPs of $NaGdF_4$:20%Yb^{3+}/2%Er^{3+}@Ag (spectrum d) manifests luminescent quenching largely, maybe due to the missing spacer which provides an indispensable separation distance between luminescent center Er^{3+} and metallic nanostructure which could prevent the absorption of Ag shell, and the complex synthesis process of Ag shell on bare core UCNPs introduces a few lattice defect on the UCNPs surface, also led to quenching to some extent.[27] Luminescence photographs of representative samples in deionized water (5 mg mL^{-1}) under 980 nm excitation suggest a visual understanding on the above presentation (inset of Fig. 4).

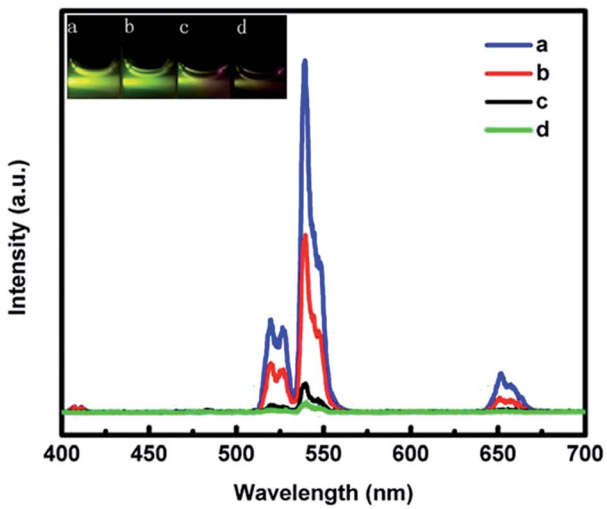

Fig. 4 Upconversion luminescence spectra of core–spacer–shell UCNPs (a), core–spacer UCNPs (b), core UCNPs (c), and core–shell UCNPs (d) in deionized water (5 mg mL^{-1}) excited by 980 nm CW laser. Inset: photographs of UC emission of (a–d). 980 nm CW laser was used as the excitation source.

2.3. Enhancement mechanism of $NaGdF_4$:20%Yb^{3+}/2% Er^{3+}@$NaGdF_4$@Ag UCNPs

To shed more light on the enhancement mechanism of up-converting luminescence in UCNPs, lifetimes of the four UCNPs at 540 nm are presented in Fig. 5. The emission decay curves of our samples with (spectrum b) and without (spectrum c) $NaGdF_4$ protective spacer indicate an increased lifetime in the presence of $NaGdF_4$ spacer, which is increased from 84.35 μs to 117.83 μs. This effect is attributed to the shielding effect of homogeneous coating spacer which reduces lattice defects and thus eliminates nonradiative radiations. In addition, $NaGdF_4$ spacer has the same refractive index with that of core UCNPs, leading to a higher light extraction efficiency and a higher emission.[28] By comparing the core–spacer structure (spectrum b) and core–spacer–shell structure (spectrum a), core–spacer–shell structure shows a longer lifetime (153.50 μs) which is consistent with its greater emission intensity. This increased lifetime could be attributed to shielding effect of Ag shell.

The presence of noble metallic nanostructures such as Ag has been known to modulate luminescence intensity which depends on separation distance between metallic nanostructure and luminescence center. Based on this mature theoretical system about LSPR, interactions between metallic nanostructure and luminescent centers which have influence on emission to a varying extent can be summarized in three

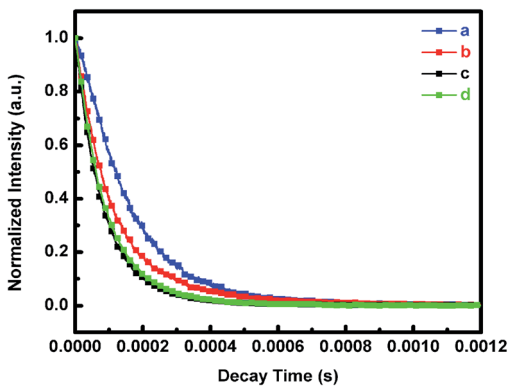

Fig. 5 Luminescence decay curves of core–spacer–shell UCNPs (a), core–spacer UCNPs (b), core UCNPs (c), and core–shell UCNPs (d), excited by OPO (λ_{ex} = 980 nm).

kinds of mode: (1) local electric field amplification which causes enhanced excitation efficiency and thus increase emission intensity; (2) enhanced radiative decay rate which causes increased quantum yield and thus increases emission intensity; and (3) energy transfer from luminescence center to metal nanoparticles which introduces an additional nonradiative deactivation channel and reduces emission intensity.[29] Among these, mode (2) and (3) certainly will give rise to the decrease of luminescent lifetime,[30] however, we do not observe this phenomenon in our study (Fig. 5, spectra c *vs.* spectra a) and instead achieve longer lifetime in core–spacer–shell UCNPs caused by the shielding effect from Ag shell and homogeneous coating.

In order to eliminate the uncertainty, we also investigate the effect of Ag shell solely (Fig. 5, spectra c *vs.* spectra d) and find that the structures of only Ag shell hardly influence luminescent lifetime (90.87 μs) however quench the emission largely. Because the complex synthesis of Ag shells on bare core UCNPs introduces a few lattice defects to the UCNPs surface and fails to provide shielding effect given the thin structure. Also Ag shells re-absorb the emission largely in the direct-contacted core–shell UCNPs. Taken together, we eliminate the possibility of enhancement mechanism of mode (2) or (3) and have reason for speculating that enhancement in emission mainly comes from local electric field amplification by Ag [mode (1)].

In order to verify the enhancement mechanism more, simulation image of the electric field amplification in core–spacer–shell UCNPs by FDTD method is given in Fig. S4.† It shows the electric field intensity enhancement at 980 nm, and the incident field is enhanced near the periphery of UCNPs (color bar indicates E/E_0). If no other factors were at play, we would expect the field enhancement to result in a 4 × 4 enhancement in emission intensity.

Meanwhile we are willing to investigate the absorption change of hollow Ag shell structure in our UCNPs system to suggest the existence of LAPR of Ag shell,[31] however, it is highly impossible for us to synthesize such a hollow structure according to the existing experimental conditions, so we adopt the FDTD method to simulate the absorption of such structure and compare it to real absorption measured in our core–spacer–shell UCNPs. As shown in Fig. S5,† there is a ~40 nm (from 565 nm to 605 nm) redshift of absorption peaks from hollow Ag shell to Ag shell in core–spacer–shell UCNPs, suggesting that the existence of plasmonic effect in our study.

From all the discussion above, we have faith in speculating that the major enhancement in our work comes from the elimination of lattice defects through the shielding effect of homogenous coating and Ag shell. LSPR of Ag shell also greatly contributes to the enhancement mechanisms owing to local electric field amplification.

3. Conclusions

Taken together, we have successfully designed and fabricated up-converting nanoparticles with a novel core–spacer–shell structure of $NaGdF_4$:Yb^{3+}/Er^{3+}@$NaGdF_4$@Ag, showing an enhanced emission arising from homogeneous coating of $NaGdF_4$ and localized surface plasmon resonance of Ag shell. The enhancement factors are up to ~12.16 fold and ~11.87 fold at 540 nm and 650 nm respectively. The enhancement comes from the elimination of lattice defects. And LSPR of Ag shell also contributes to the enhancement stemming from local electric field amplification which causes enhanced excitation efficiency and thus enhanced emission intensity to a great extent.

4. Experimental section

4.1. Chemicals and materials

Rare earth oxides (Gd_2O_3, Yb_2O_3, Er_2O_3, 99.99%) were purchased from Science and Technology Parent Company of Changchun Institute of Applied Chemistry. Oleic acid (OA; >90%) and 1-octadecene (ODE; >90%) were purchased form Sigma-Aldrich. Sodium citrate, ascorbic acid (AA), silver nitrate ($AgNO_3$), thioglycollic acid (TGA), ammonium fluoride (NH_4F), sodium hydroxide (NaOH) and organic solvents (ethanol, methanol, diethyl ether, and acetone) were purchased from Beijing Chemical Works. All above chemical reagents were analytical grade and used as received without further purification. Rare earth salts ($GdCl_3 \cdot 6H_2O$, $YbCl_3 \cdot 6H_2O$, $ErCl_3 \cdot 6H_2O$) were prepared by dissolving corresponding rare earth oxides (Gd_2O_3, Yb_2O_3, Er_2O_3, 99.99%) in hydrochloric acid and evaporating their solutions.

4.2. Characterization

Scanning electronic microscopy (SEM) images and EDX spectrometry were recorded on a Hitachi S-4800 microscope. Transmission electron microscopy (TEM) images and elemental mapping were taken with a JEM-2010 transmission election microscope made by Japanese JEOL Company. Dynamic light scattering measurements (DLS) was performed on Brookhaven Instruments Corporation ZetaPALS. Powder X-ray diffraction (XRD) patterns were recorded on a Bruker D4 X-ray diffractometer (Germany) with Ni-filtered Cu K radiation (40 kV, 30 mA). Optical measurements were acquired on a Hitachi F-4500 fluorescence spectrophotometer under the excitation of a 980 nm laser diode. Luminescent lifetime curves were obtained on a fluorescence lifetime measurement system with an optical parametric oscillator (OPO) as excitation source and a Tektronix digital oscilloscope (TDS 3052) as signal detector. Fourier-transform infrared (FT-IR) spectra were collected on a Nicolet Fourier spectrophotometer using KBr pellets. UV-vis absorption spectra were obtained on a Shimadzu-UV-3101 scanning spectrophotometer. Both up-converting luminescence spectra and luminescent lifetime were performed with sample dispersion (5 mg mL^{-1}) in deionized water. Sample b and sample c were modulated by hydrochloric solution with pH = 4–5 to detach surface OA, and then well dispersed in deionized water for further measurement.

4.3. Synthesis of β-$NaYF_4$:20%Yb^{3+}/2%Er^{3+} UCNPs

In a typical procedure,[6] $GdCl_3 \cdot 6H_2O$ (0.5798 g), $YbCl_3 \cdot 6H_2O$ (0.1550 g), $ErCl_3 \cdot 6H_2O$ (0.0152 g), OA (12 mL) and ODE (30 mL) were added to a 100 mL flask. The solution was stirred at 150 °C

for 30 min to form a well-proportioned solution. After natural cooling, a methanol solution (10 mL) containing NH_4F (0.308 g) and NaOH (0.2 g) was dropwise added to the flask and stirred vigorously at 40 °C for 30 min. Then temperature was elevated to 70 °C to remove methanol within a period of 30 min. After that, the solution was heated to 300 °C rapidly and maintained for 1.5 h. Then it was cooled to room temperature naturally. Nitrogen protection was maintained throughout the entire process. Crude products were precipitated by adding acetone, and washed with ethanol and deionized water for three times. Finally, products were dried in vacuum oven for 12 h, and weighed accurately for further experiments.

4.4. Synthesis of $NaGdF_4$:20%Yb^{3+}/2%Er^{3+}@$NaGdF_4$ UCNPs

Similar to the synthesis described above, $NaGdF_4$:Yb^{3+}/Er^{3+}@$NaGdF_4$ nanoparticles were prepared by heating and stirring the mixture of $GdCl_3 \cdot 6H_2O$ (0.298 g), OA (12 mL) and ODE (30 mL) at 150 °C for 30 min in a 100 mL flask. The obtained $NaGdF_4$:20%Yb^{3+}/20%Er^{3+} core nanoparticles (0.2 g) dispersed in cyclohexane (5 mL) were used as seeds and added dropwise into the solution. After natural cooling, a methanol solution (10 mL) containing NH_4F (0.124 g) and NaOH (0.08 g) was added to the flask and stirred at 40 °C vigorously for 30 min. Then temperature was elevated to 90 °C to remove methanol and cyclohexane within a period of 30 min. After that, the mixture was heated to 300 °C rapidly and maintained for 1.5 h. Then it was cooled to room temperature naturally. This entire process was under nitrogen protection. The products were manipulated following an identical procedure mentioned in Section 4.3.

4.5. Synthesis of $NaGdF_4$:Yb^{3+}/Er^{3+}@$NaGdF_4$@Ag UCNPs

To get rid of OA on sample surface, $NaGdF_4$:Yb^{3+}/Er^{3+}@$NaGdF_4$ nanoparticles were re-dispersed and stirred vigorously in 15 mL of hydrochloric acid solution at pH within 4–5 for 24 h. After that, detached OA was extracted with diethyl ether (30 mL) for several times. The UCNPs products in aqueous phase were reserved and then washed with mixed solution of deionized water/acetone (v/v = 1 : 10) for three times. Thioglycolic acid (TGA, 2 mL) in 18 mL of water was mixed with the UCNPs colloid. After being stirred for 48 h, the UCNPs were purified by centrifugation, washed several times with deionized water and ethanol, and then re-dispersed in deionized water for further use.

Above UCNPs solution was stirred and mixed with sodium citrate solution (4 mL, 10 wt%). Two hours later, $AgNO_3$ solution (0.015 M, 10 mL) was added under gentle stirring for an hour. Finally, 1 mL of ascorbic acid solution (AA, 15 wt%) was injected into the above solution. The reaction started immediately and lasted for 5 min. Crude product was washed with ethanol and deionized water for three times. Finally, this product was dried in the vacuum oven for 12 h, and weighed accurately for further experiments.

4.6. Synthesis of $NaGdF_4$:Yb^{3+}/Er^{3+}@Ag UCNPs

To get rid of OA on sample surface, Yb/Er-codoped core UCNPs with OA on the surface were dispersed and stirred vigorously in 15 mL of hydrochloric acid solution at pH within 4–5 for 24 h. After that, detached OA was extracted with diethyl ether (30 mL) for several times. The UCNPs products in aqueous phase were reserved and then washed with mixed solution of deionized water/acetone (v/v = 1 : 10) for three times. Thioglycolic acid (TGA, 2 mL) in 18 mL of water was mixed with the UCNPs colloid. After being stirred for 48 h, the UCNPs were purified by centrifugation, washed several times with deionized water and ethanol. Above UCNPs was mixed with sodium citrate aqueous solution (4 mL, 10 wt%) under stirring. Two hours later, $AgNO_3$ solution (0.015 M, 10 mL) was added under gentle stirring for an hour. Finally, 1 mL of ascorbic acid solution (AA, 15 wt%) was injected into the above solution. The reaction started immediately and lasted for 5 min. Crude product was washed with ethanol and deionized water for three times and dried in the vacuum oven for 12 h.

Acknowledgements

The authors gratefully thank the financial supports of the NSFC (Grant No. 51372240, 51572256, 21501166).

Notes and references

1 H. Aouani, M. Rahmani, M. Navarro-Cia and S. A. Maier, *Nat. Nanotechnol.*, 2014, **9**, 290–294.
2 V. Gray, D. Dzebo, M. Abrahamsson, B. Albinsson and K. Moth-Poulsen, *Phys. Chem. Chem. Phys.*, 2014, **16**, 10345–10352.
3 D. J. Gargas, E. M. Chan, A. D. Ostrowski, S. Aloni, M. V. Altoe, E. S. Barnard, B. Sanii, J. J. Urban, D. J. Milliron, B. E. Cohen and P. J. Schuck, *Nat. Nanotechnol.*, 2014, **9**, 300–305.
4 G. Chen, H. Qiu, P. N. Prasad and X. Chen, *Chem. Rev.*, 2014, **114**, 5161–5214.
5 G. Yi, H. Lu, S. Zhao, Y. Ge, W. Yang, D. Chen and L.-H. Guo, *Nano Lett.*, 2004, **4**, 2191–2196.
6 J. Zhang, B. Li, L. Zhang and H. Jiang, *Chem. Commun.*, 2012, **48**, 4860–4862.
7 R. Abdul Jalil and Y. Zhang, *Biomaterials*, 2008, **29**, 4122–4128.
8 L. Yang and Y. Li, *Analyst*, 2006, **131**, 394–401.
9 S. Stolik, J. A. Delgado, A. Pérez and L. Anasagasti, *J. Photochem. Photobiol., B*, 2000, **57**, 90–93.
10 C. Salthouse, S. Hildebrand, R. Weissleder and U. Mahmood, *Opt. Express*, 2008, **16**, 21731–21737.
11 F. Wang and X. Liu, *Chem. Soc. Rev.*, 2009, **38**, 976–989.
12 P. Yuan, Y. H. Lee, M. K. Gnanasammandhan, Z. Guan, Y. Zhang and Q. H. Xu, *Nanoscale*, 2012, **4**, 5132–5137.
13 F. Wang, J. Wang and X. Liu, *Angew. Chem.*, 2010, **49**, 7456–7460.

14 P. T. Burks, J. V. Garcia, R. GonzalezIrias, J. T. Tillman, M. Niu, A. A. Mikhailovsky, J. Zhang, F. Zhang and P. C. Ford, *J. Am. Chem. Soc.*, 2013, **135**, 18145–18152.
15 G. Chen, C. Yang and P. N. Prasad, *Acc. Chem. Res.*, 2013, **46**, 1474–1486.
16 J. Wang, R. Deng, M. A. MacDonald, B. Chen, J. Yuan, F. Wang, D. Chi, T. S. Hor, P. Zhang, G. Liu, Y. Han and X. Liu, *Nat. Mater.*, 2014, **13**, 157–162.
17 F. Zhang, G. B. Braun, Y. Shi, Y. Zhang, X. Sun, N. O. Reich, D. Zhao and G. Stucky, *J. Am. Chem. Soc.*, 2010, **132**, 2850–2851.
18 N. J. Greybush, M. Saboktakin, X. Ye, C. Della Giovampaola, S. J. Oh, N. E. Berry, N. Engheta, C. B. Murray and C. R. Kagan, *ACS Nano*, 2014, **8**, 9482–9491.
19 W. Park, D. Lu and S. Ahn, *Chem. Soc. Rev.*, 2015, **44**, 2940–2962.
20 Y. Ding, X. Zhang, H. Gao, S. Xu, C. Wei and Y. Zhao, *J. Lumin.*, 2014, **147**, 72–76.
21 W. Feng, L. D. Sun and C. H. Yan, *Chem. Commun.*, 2009, 4393–4395.
22 M. Saboktakin, X. Ye, U. K. Chettiar, N. Engheta, C. B. Murray and C. R. Kagan, *ACS Nano*, 2013, **7**, 7186–7192.
23 W. Niu, H. Chen, R. Chen, J. Huang, A. Palaniappan, H. Sun, B. G. Liedberg and A. I. Tok, *Small*, 2014, **10**, 3637–3643.
24 B. Dong, S. Xu, J. Sun, S. Bi, D. Li, X. Bai, Y. Wang, L. Wang and H. Song, *J. Mater. Chem.*, 2011, **21**, 6193.
25 C. Zhong, P. Yang, X. Li, C. Li, D. Wang, S. Gai and J. Lin, *RSC Adv.*, 2012, **2**, 3194.
26 H.-X. Mai, Y.-W. Zhang, R. Si, Z.-G. Yan, L.-d. Sun, L.-P. You and C.-H. Yan, *J. Am. Chem. Soc.*, 2006, **128**, 6426–6436.
27 W. Deng, L. Sudheendra, J. Zhao, J. Fu, D. Jin, I. M. Kennedy and E. M. Goldys, *Nanotechnology*, 2011, **22**, 325604.
28 Q. Su, S. Han, X. Xie, H. Zhu, H. Chen, C. K. Chen, R. S. Liu, X. Chen, F. Wang and X. Liu, *J. Am. Chem. Soc.*, 2012, **134**, 20849–20857.
29 D. M. Wu, A. Garcia-Etxarri, A. Salleo and J. A. Dionne, *J. Phys. Chem. Lett.*, 2014, **5**, 4020–4031.
30 H. Zhang, Y. Li, I. A. Ivanov, Y. Qu, Y. Huang and X. Duan, *Angew. Chem.*, 2010, **49**, 2865–2868.
31 X. Chen, W. Xu, L. Zhang, X. Bai, S. Cui, D. Zhou, Z. Yin, H. Song and D.-H. Kim, *Adv. Funct. Mater.*, 2015, **25**, 5462–5471.